Propulsion and Power Research 2022;11(3):293–310

http://ppr.buaa.edu.cn/

Propulsion and Power Research

www.sciencedirect.com

REVIEW

A review of cooling technologies for high temperature rotating components in gas turbine

Umesh Unnikrishnan, Vigor Yang*

Georgia Institute of Technology, Atlanta, GA, USA

Received 10 June 2022; accepted 17 June 2022
Available online 1 August 2022

KEYWORDS

Gas turbine;
Rotating components;
Turbine blade;
Turbine disk;
Cooling technology

Abstract Modern gas turbines work under demanding high temperatures, high pressures, and high rotational speeds. In order to ensure durable and reliable operation, effective cooling measures must be applied to the high-temperature rotating components, including turbine blades and turbine disks. Cooling technology, however, is one of the most challenging problems in this field. The present work reviews the current state of cooling technology research, at both the fundamental science and engineering implementation levels, including modeling and simulation, experiments and diagnostics, and cooling technologies for blades and disks. In numerical simulation, the RANS approach remains the most commonly used technique for flow-dynamics and heat-transfer simulations. Much attention has been given to the development of improved turbulence modeling for flows under rotation. For measurement and diagnostics, advanced instrumentation and rotating-flow test facilities have been developed and valuable experimental data obtained. Detailed velocity and temperature distributions in rotating boundary layers have been obtained at scales sufficient to resolve various underlying mechanisms. Both isothermal and non-isothermal conditions have been considered, and the effects of Coriolis and buoyancy forces on flow evolution and heat transfer quantitatively identified. Cooling technologies have been improved by optimizing cooling passage dsigns, especially for curved configurations under rotation. Novel methods such as lamellar cooling and micro-scale cooling were proposed,

*Corresponding author.
E-mail address: vigor.yang@aerospace.gatech.edu (Vigor Yang).
Peer review under responsibility of Propulsion and Power Research.

ELSEVIER Production and Hosting by Elsevier on behalf of KeAi

https://doi.org/10.1016/j.jppr.2022.07.001

and their effectiveness evaluated. For disk/cavity cooling, efforts were mainly focused on rotor-stator systems, with special attention given to the position of air injection into disks.

Nomenclature

$\boldsymbol{V}$	velocity vector (unit: m/s)
$\boldsymbol{\Omega}$	angular velocity vector (unit: rad/s)
$\boldsymbol{r}$	radius vector (unit: m)
ρ	density (unit: kg/m^3)
μ	dynamic viscosity (unit: Pa·s)
α	thermal diffusion coefficient (unit: m^2/s)
β	volume expansion coefficient (unit: 1/K)
y^+	dimensionless distance
u^+	dimensionless velocity
q	heat flux (unit: W/m^2)
T_w	local average temperature (unit: K)
T_c	cooling gas temperature (unit: K)

1. Introduction

In the long and complex evolution of gas turbines, effective cooling of turbine components has been and remains a challenging issue, and it dictates the efficiency and operation of the entire system. Significant progress has been made in recent decades in aero and mechanical designs, materials integrity, manufacturing technology, and testing and evaluation techniques. Turbine inlet temperatures (TIT) have continued to increase, and now far exceed the allowable working temperatures of typical turbine components, such as guide vanes, blades, and disks. The cooling of rotational components is therefore a major topic in gas turbine engineering and research, and entails several specific challenges. The continuous rotation of such components induces mechanical stress, leading to fatigue and reduced life span. The flow dynamics of cooling channels and films associated with these components is complicated by rotation-induced Coriolis and buoyancy forces. From the research and development perspective, rotational flows also pose severe challenges for development of suitable measurement techniques.

Significant progress has been achieved in the past few decades in these areas through numerical and experimental campaigns. The scientific and technological bases of turbine heat transfer and cooling, as well as advances through 2010, were given by Han et al. [1], and a comprehensive review of the state of the art prior to 2014 can be found in the volume compiled by Shih and Yang [2]. Owen and Christopher [3] reviewed the cooling technologies for turbine cavities in 2015. Acharya and Kanani [4] reviewed the film cooling technologies for turbine blades in 2017. This paper presents a broad review of recent advances in cooling technologies for rotating components in gas turbines. Special attention is devoted to the development of fundamental theories and the understanding of the underlying flow physics. The challenges and advances in developing modeling and experimental capabilities, at resolutions sufficient to describe the local and global behaviors of fluid flows and heat transfer, especially under high-temperature, rotating environments, are discussed.

2. Basic theories of fluid flow and heat transfer under rotation

A turbine rotates in a high-temperature environment following the fundamental conservation laws for mass, momentum and energy. Researchers, however, choose different forms of the governing equations for different components to simplify the formulation of particular problems. Generally, equations are expressed in a non-inertial, rotating coordinate system for turbine blades, while an inertial stationary coordinate system in cylindrical form is selected for turbine disks, mainly due to their circumferential geometric symmetry.

For turbine blades, the steady-state governing equations under a rotating coordinate system in vector form can be written as:

Continuity equation:

$$\nabla.(\rho \boldsymbol{V}) = 0 \tag{1}$$

Momentum equation:

$$\begin{aligned}\rho(\boldsymbol{V} \cdot \nabla)\boldsymbol{V} = &-\nabla P + \mu\nabla^2\boldsymbol{V} - \rho[2\boldsymbol{\Omega}\times\boldsymbol{V} + \boldsymbol{\Omega}\times(\boldsymbol{\Omega}\times\boldsymbol{z})] \\ &+ \rho\beta[2\boldsymbol{\Omega}\times\boldsymbol{V} + \boldsymbol{\Omega}\times(\boldsymbol{\Omega}\times\boldsymbol{z})]\Delta T\end{aligned} \tag{2}$$

Energy equation:

$$(\boldsymbol{V} \cdot \nabla)T = \alpha\nabla^2 T \tag{3}$$

where $\boldsymbol{V}$ is the velocity vector in the rotating frame of reference, $\boldsymbol{\Omega}$ is the angular velocity of the reference frame, and β is the coefficient of thermal expansion. Boussinesq approximation is applied in the momentum Eq. (2) to model the density variation due to temperature change. Further, it is considered that heat transfer due to conduction and convection are the most dominant effects, and the viscous dissipation term is neglected in Eq. (3).

Compared to the governing equations in a stationary frame of reference, three non-inertial terms are included in the momentum equation. These are $-\rho\boldsymbol{\Omega}\times(\boldsymbol{\Omega}\times\boldsymbol{z})$,

$-\rho(2\boldsymbol{\Omega}\times\boldsymbol{V})$, and $\rho\beta[2\boldsymbol{\Omega}\times\boldsymbol{V}+\boldsymbol{\Omega}\times(\boldsymbol{\Omega}\times z)]\Delta T$, representing the centrifugal force, Coriolis force, and buoyant force respectively, and together representing the non-inertial effects. These terms make the study of flow and heat transfer processes very complicated. The Coriolis force always acts perpendicular to the velocity and gives rise to a secondary flow. The buoyant force depends heavily on the temperature field, and so closely couples the momentum and energy equations. The buoyant force plays an important role in turbine environments due to the high rotational speeds and presence of high temperature gradients.

For turbine disks and/or cavities, the steady-state governing equations in cylindrical form are used, and can be written as:

Continuity equation:

$$\rho\frac{\partial v}{r\partial r}+\rho\frac{\partial w}{r\partial\theta}+\rho\frac{\partial u}{\partial z}=0 \tag{4}$$

Momentum equations:

$$\begin{aligned}\frac{\partial(ruv)}{r\partial r}+\frac{\partial(uw)}{r\partial\theta}+\frac{\partial(uu)}{\partial z}= &-\frac{1}{\rho}\frac{\partial p}{\partial z}+\frac{1}{\rho}\frac{\partial}{r\partial r}\left[\mu r\left(\frac{\partial v}{\partial z}+\frac{\partial u}{\partial r}\right)\right]\\ &+\frac{1}{\rho}\frac{\partial}{r\partial\theta}\left[\mu\left(\frac{\partial w}{\partial z}+\frac{\partial u}{r\partial\theta}\right)\right]\\ &+\frac{1}{\rho}\frac{\partial}{\partial z}\left[2\mu\left(\frac{\partial u}{\partial z}\right)\right]\end{aligned} \tag{5}$$

$$\begin{aligned}\frac{\partial(rvv)}{r\partial r}+\frac{\partial(wv)}{r\partial\theta}+\frac{\partial(vu)}{\partial z}= &-\frac{1}{\rho}\frac{\partial p}{\partial r}+\frac{1}{\rho}\frac{2\partial}{r\partial r}\left[\mu r\frac{\partial v}{\partial r}\right]\\ &+\frac{1}{\rho}\frac{\partial}{r\partial\theta}\left[\mu\left(\frac{\partial v}{r\partial\theta}+\frac{\partial w}{\partial r}-\frac{w}{r}\right)\right]+\frac{1}{\rho}\frac{\partial}{\partial z}\left[\mu\left(\frac{\partial v}{\partial z}+\frac{\partial u}{\partial r}\right)\right]\\ &-\frac{1}{\rho}\frac{2\mu}{r}\left(\frac{\partial w}{r\partial\theta}+\frac{v}{r}\right)+(1-\beta\,\Delta T)\left(\frac{w^2}{r}+\omega^2 r+\omega w\right)\end{aligned} \tag{6}$$

$$\begin{aligned}\frac{\partial(rvw)}{r\partial r}+\frac{\partial(ww)}{r\partial\theta}+\frac{\partial(wu)}{\partial z}= &-\frac{1}{\rho}\frac{\partial p}{r\partial\theta}+\frac{1}{\rho}\frac{\partial}{r\partial r}\left[\mu r\left(\frac{\partial w}{\partial r}+\frac{\partial v}{r\partial\theta}\right.\right.\\ &\left.\left.-\frac{w}{r}\right)\right]+\frac{1}{\rho}\frac{\partial}{r\partial\theta}\left[\mu\left(\frac{2\partial w}{r\partial\theta}+\frac{2v}{r}\right)\right]+\frac{1}{\rho}\frac{\partial}{\partial z}\left[\mu\left(\frac{\partial w}{\partial z}+\frac{\partial u}{r\partial\theta}\right)\right]\\ &+\frac{1}{\rho}\frac{\mu}{r}\left(\frac{\partial v}{r\partial\theta}+\frac{\partial w}{\partial r}-\frac{w}{r}\right)+(1-\beta\Delta T)\left(-\frac{wv}{r}-2\omega v\right)\end{aligned} \tag{7}$$

Energy equation:

$$\begin{aligned}\frac{\partial(rvT)}{r\partial r}+\frac{\partial(wT)}{r\partial\theta}+\frac{\partial(uT)}{\partial z}= &\frac{\partial}{\rho r\partial r}\left(\frac{r\lambda}{c_p}\frac{\partial T}{\partial r}\right)\\ &+\frac{\partial}{\rho r\partial\theta}\left(\frac{\lambda}{c_p}\frac{\partial T}{r\partial\theta}\right)+\frac{1}{\rho}\frac{\partial}{\partial z}\left(\frac{\lambda}{c_p}\frac{\partial T}{\partial z}\right)\end{aligned} \tag{8}$$

In a cylindrical coordinate system, additional Coriolis force terms, ωw in r and $-2\omega v$ in θ, and buoyant force: $-\beta\Delta T\left(\frac{w^2}{r}+\omega^2 r+\omega w\right)$ in r and $\beta\Delta T\left(\frac{wv}{r}+2\omega v\right)$ in θ, also appear, due to the existence of curvature velocity, even though the coordinate is stationary. ω is the rotational speed of the disk.

The above sets of equations are often used in numerical simulations, design of experimental facilities, and data analysis. The existence of Coriolis force and buoyant force terms, in both rotating coordinate systems for turbine blades and stationary cylindrical coordinate systems for rotating disks, is the most significant feature of interest. Rotation makes the flow and heat transfer phenomena in turbine blades and turbine disks very complex, and imposes requirements for specialized turbulence models for numerical simulations, and sophisticated test facilities equipped with advanced diagnostics and measurement techniques for experimental work.

3. Developments in numerical simulation

Numerical simulation has long been an important way to provide detailed flow information for the study of flow and heat transfer problems pertaining to rotating turbine components. Advancements in computing hardware and software technologies over the past two decades, however, have opened opportunities to solve complex 3D problems that require large computing power. Computational fluid dynamics (CFD) and numerical heat transfer (NHT) have undergone significant advancements: many fast and accurate algorithms have been developed, and better turbulence models have been proposed. Numerical simulation is playing an increasingly significant role in the study of rotational flow and heat transfer.

Numerical simulation of turbulent flows can be broadly classified into three categories: direct numerical simulation (DNS), large eddy simulation (LES), and Reynolds averaged Navier-Stokes (RANS) modeling. Though computing power has increased tremendously, the RANS method is still the dominant approach for large scale engineering simulation, including fluid flow and heat transfer within high temperature turbine rotating components in complex geometries. DNS and LES are limited to highly simplified geometries and studies on fundamental flow and heat transfer mechanisms. It is expected that the use of LES and/or DNS to simulate complex engineering problems will become more feasible in the future, as computing power continues to increase.

Turbulence modeling is an important focal point for the development of the RANS methodology, and to a large extent determines the accuracy of numerical simulations. Over the years, a variety of turbulence models have been developed, and the RANS method continues to evolve and mature in terms of accuracy and robustness. Different turbulence models have distinct advantages and limitations for different sets of operating conditions, and a thorough understanding of various models is imperative for an effective study. In this section, we discuss representative research related to rotating fluid flow and heat transfer.

In early numerical studies of film cooling, the method of solving the two-dimensional boundary layer equations was mainly employed [5−8]. With increase in computing power, three-dimensional simulation of film cooling has become increasingly popular. Leylek and Zerkle [9] used the *k*-epsilon model to predict jet-impingement air film cooling of discrete jet holes on flat plates, and compared the numerical results with experimental results to understand the interaction between a jet and transverse flow in discrete jet-impingement air film cooling. The simulation illustrates important aspects of film cooling, such as the structure of symmetric secondary vortices in transverse flow. Sivriolu's study [10] showed that the cooling effect of a suction surface is better than that of a flat surface. The effect of pressure surface cooling is lower than that of plate cooling, and the effect of a pressure gradient on film cooling of a curved surface is higher than that of plate cooling on the same surface.

Howard et al. [11] derived the *k*-epsilon model, including the effect of the Coriolis force term, for flow in a rotating rectangular channel. Prakash and Zerkle [12] used the standard *k*-epsilon model to conduct three-dimensional numerical simulation of the rotating rectangular channel, by also taking into account the influence of Coriolis force and centrifugal force caused by rotation and emphasized that the buoyancy force has a strong influence on the flow and heat transfer. Dutta et al. [13] adopted a modified *k*-epsilon model to conduct numerical simulation of the flow and heat transfer in a rotating rectangular channel. The model includes a modification of the *k*-epsilon two equation system that incorporates the Coriolis force and centrifugal buoyant force induced by rotation and wall heat transfer. Due to the velocity distribution within the boundary layer, the influence of the modified term of the Coriolis force in the boundary region was considered far greater than that of the off-center uplift force. The influence of the off-center uplift force was found to be less than 5% in the case of radial outflow. This study also predicted that separation at the leading edge would lead to increased turbulence intensity, and thus enhance the heat transfer at the leading edge. Tao and colleagues [14] proposed a new rotational-modification method based on the *k*-omega model, constructing the anisotropic eddy viscosity tensor deduced from the Reynolds stress equations including the Coriolis force term. Comparison of their model with the standard *k*-omega model indicates that their prediction is more accurate for the case of a rotating square channel.

4. Measurement techniques

Measurement techniques for flow and heat transfer characteristics in stationary setups are well developed. The deployment of these techniques for their rotating counterparts, however, poses a number of challenges, including the selection and installation of sensors. Furthermore, the harsh electromagnetic environment created by the rotation of the blades inhibits signal transmission. As a result, very few institutions have been successful in establishing relevant experimental facilities, and experimental research in this area has been limited.

4.1. Measurement of the rotating velocity field

The state-of-the-art measurement methods for the velocity field under a rotating state are: hot-wire anemometry, particle image velocimetry (PIV), laser doppler velocimetry (LDV), phase doppler particle analysis (PDPA), computed tomography (CT), and planar laser-induced fluorescence (PLIF). Hot wire anemometry is a mature measurement technique. Being a single point, contact measurement method, its advantage over other methods lies in its higher measuring frequency. This method is also not prone to the reflection issues that are often encountered in optical methods. Hence, the hot wire anemometry technique is well-suited for measurements near the wall boundaries. In recent years, Tao and colleagues [15−17] modified the hot wire anemometer to make it suitable for measuring the rotating boundary layer, as shown in Figure 1. With this method the velocity and the temperature distributions can be measured simultaneously. The work is of milestone significance. It is an important step forward that provides unique opportunities for exploring the detailed mechanisms of fluid flow and heat transfer within the rotating boundary layer. Various underlying flow physics are resolved at scales ($y^+<3$) sufficient to identify the key processes and mechanisms throughout the entire boundary layer.

In contrast to hot wire anemometry, PIV can realize measurement of the complete velocity field, and has been widely adopted by scholars. However, it entails major challenges under the rotating state. Arts et al. [18−20] were pioneers in adapting equipment such as time-resolved PIV, high-frequency cameras, and continuous lasers to perform velocity field measurements under rotating conditions, with a remarkable sampling frequency as high as 1550 Hz, as shown in Figure 2. Owen [21], Ong and Owen [22], and Wei et al. [23] employed similar PIV techniques to measure the velocity in the rotating disk cavity and rotating channel respectively.

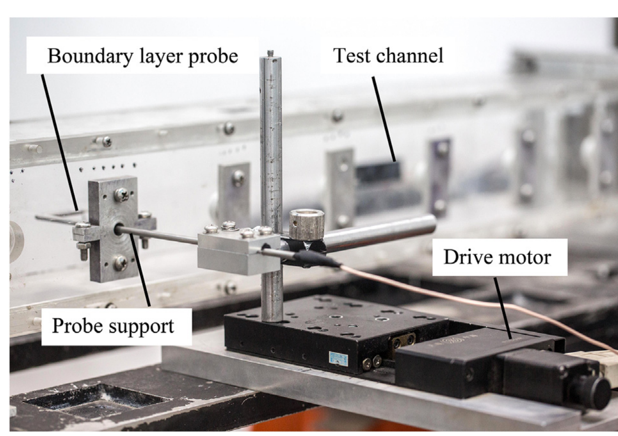

Figure 1 Rotary hot wire equipment adapted by Tao and colleagues [15−17].

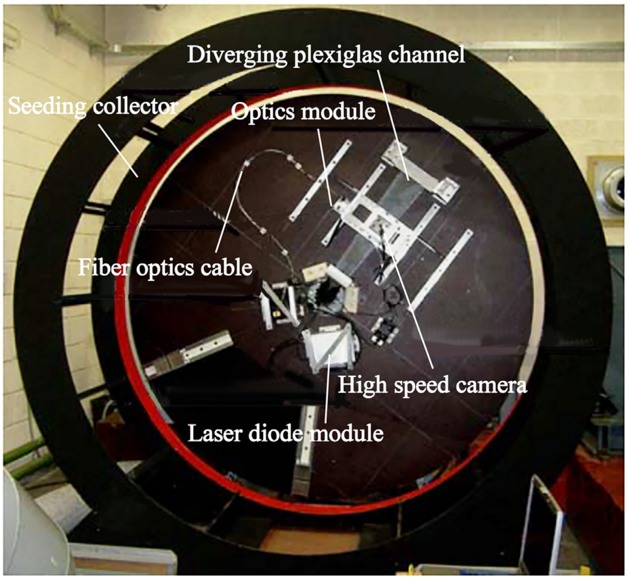

Figure 2 Rotating TR-PIV equipment adapted by Arts and colleagues [18−20].

LDV is another non-intrusive technique for measuring velocities, and it offers the advantage of higher measurement frequency. Liou et al. [24] utilized LDV to measure the flow in a rotating channel, as shown in Figure 3, and conducted spectral analysis of the turbulent fluctuations in the channel with LDV data. LDV and PDPA techniques are based on the doppler effect and allow the simultaneous single-point measurement of the size and velocity of spherical particles, droplets, and bubbles.

Computed tomography (CT) is an imaging technique that can effectively overcome the limitations of planar imaging techniques. CT is often combined with optical imaging principles such as optical interference [25], light diffraction [26], spectral absorption [27], chemiluminescence [28], and particle imaging [29] to form a variety of combustion diagnostic and visualization techniques.

Planar laser-induced fluorescence is an effective measurement technique in which fluorescent particles are dispersed in the flow to image the flow field. The fluorescence intensity in the flow field is proportional to the concentration or the local fluid density. Zhang et al. [30] used PIV and PLIF to measure time-resolved velocity and density fields of film outflow with crossflow.

4.2. *Measurement of the temperature field under rotating conditions*

There are three major methods of temperature measurement under the rotating state: thermocouple thermometry, liquid crystal thermometry (LCT), and infrared thermometry (IRT), single-short UV laser Rayleigh scattering, laser holographic interferometry (LHI), and thermographic phosphor (TP). Wagner and colleagues [31,32] and Johnson et al. [33,34] used the thermocouple method for measurements within an internal cooling turbine blade channel, as shown in Figure 4. This method, also known as the copper block method, divides the whole channel into several small sections. Each section is composed of a copper block and a heating film, with the copper plates separated by thermal insulation materials. During the experiment, the heat q can

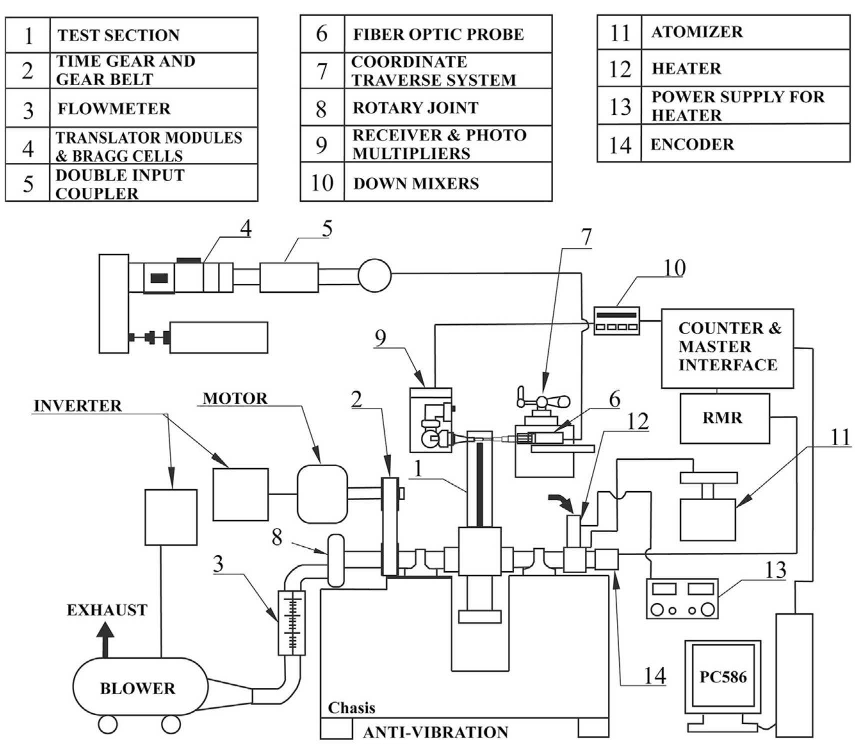

Figure 3 Rotating LDV equipment adapted by Liou and colleagues [39].

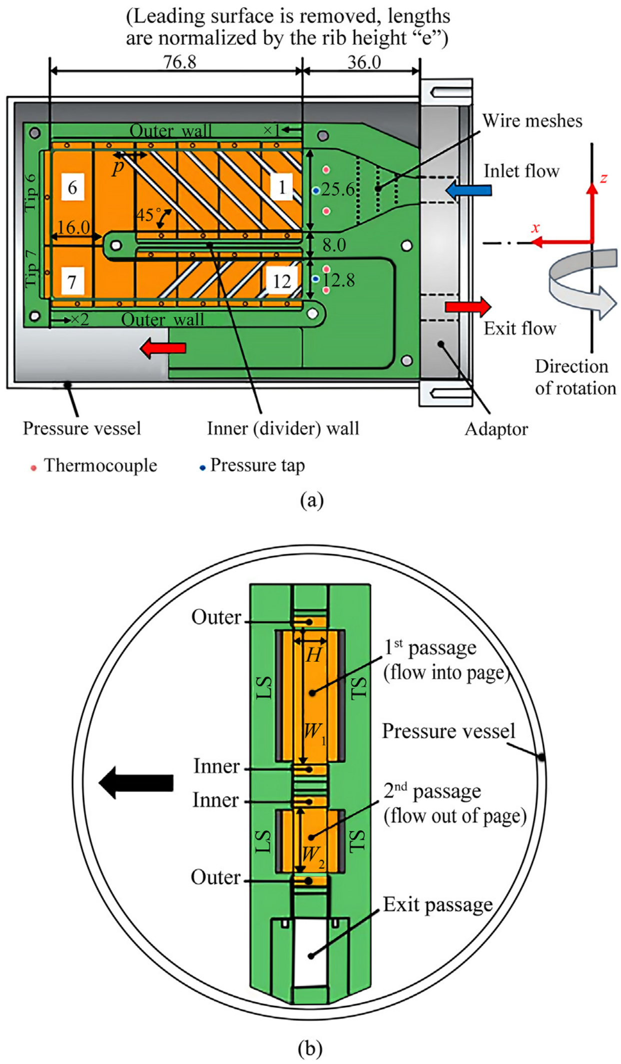

Figure 4 Schematic of technique for measurement of heat transfer coefficient by copper block method, by Wagner, Johnson, and colleagues [31−34].

be obtained by heating each copper block with a heating film, while the local average temperature T_w and the temperature of the cooling gas T_c can both be obtained by thermocouples. Thus, the wall convection heat transfer coefficient of the turbine blade cooling channel can be calculated. Although this method is a type of point temperature measurement, it is still widely used as the benchmark for rotating temperature measurement, due to its great accuracy and stability. Han et al. [1,35] employed a similar method to study the internal cooling characteristics of turbine blades under rotating conditions.

Liquid crystal thermometry is a non-contact full field measurement technique. It provides the advantages of high resolution (temperature resolution up to 0.1 °C, spatial resolution up to 1 mm), fast reaction speed, and good repeatability. Taslim et al. [36] and Ekkad et al. [37] studied the heat transfer characteristics of a ribbed channel in the rotating state and the heat transfer of the double flow channel between the rib and the film hole by using this method.

Infrared temperature measurement is also a non-contact temperature measurement technique. This technique is similar to the liquid crystal method, but features a larger temperature range. Liou and colleagues [38,39] applied it to the measurement of wall heat transfer in the internal cooling channel of a turbine blade, as shown in Figure 5.

Jin and Kim [40] used single-shot UV laser Rayleigh scattering to simultaneously measure the laminar burning velocity and two-dimensional (2D) temperature distribution inside a chamber at different equivalence ratios and initial pressures. Laser holographic interferometry (LHI) is a powerful tool used to provide insight into fluid dynamics and heat transfer processes. LHI is non-intrusive technique that uses interference fringes to realize the display of temperature field characteristics. Liou et al. [41] utilized LHI to measure time variations of the temperature distribution and scales of eddy motion of a heated rib pair-roughened channel. Thermographic phosphor (TP) is a temperature measurement technique suitable for measurements in high temperature environments. TP is a non-intrusive, non-destructive, transient response surface thermal state detection technique commonly used for aero-engine high temperature components. Alaruri et al. [42] obtained the turbine surface temperature distribution using TP, where the maximum temperature reached was 750 °C.

5. Cooling of turbine blades

With extensive efforts over the past several decades, the inlet temperatures for high-pressure turbines have increased to over 1900 K, far exceeding the allowable temperatures of turbine blade materials. Cooling has long been applied to protect blades in high-temperature environments. Various active cooling schemes, internal and external, have been developed and implemented to ensure safe and efficient operation of turbine blades. Prior to the 1960s, simple internal cooling schemes were developed and implemented. Technologies have evolved from internal passages with/without ribs, to impingement cooling, film cooling, impingement-film composite cooling, double wall cooling, to now prospective convergent cooling engaging multiple techniques. Figure 6, extended from the work of Clifford et al. [43], summarizes the development of turbine blade cooling technology over the past seven decades. It can be generally divided into two categories: internal cooling with enhanced heat transfer, and film cooling applied to external blade surfaces. Film cooling began to be incorporated into turbine blade design in the 1970s, greatly improving cooling capacity. Regardless of the cooling scheme, however, the baseline flow structure that dominates the cooling effectiveness is the boundary layer surrounding the surface of the turbine components. The present section first discusses recent advances in the understanding of rotating boundary layers under isothermal and non-isothermal conditions, and then addresses cooling schemes, internal and external, for turbine blades.

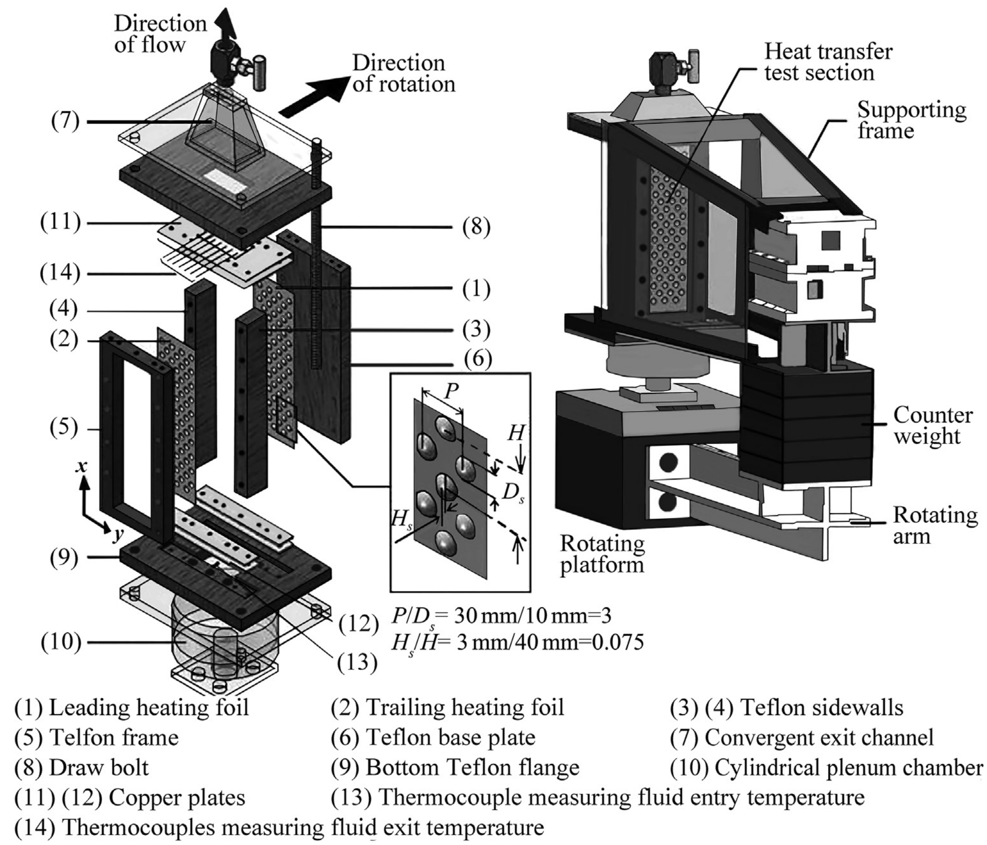

Figure 5 Schematics of the measurement setup using infrared thermometry by Liou and colleagues [38,39].

5.1. Boundary layer under rotation

The flow and heat transfer characteristics within the rotating boundary layer around the blade surface determine to a great extent the effectiveness of a blade cooling scheme. Compared with stationary blades, rotation is associated with phenomena such as asymmetric and local strengthening of heat transfer, which must be taken into account. Existing studies have focused on two broad areas of interest: isothermal boundary layers and non-isothermal boundary layers, within which temperature gradients exist.

Studies on isothermal boundary layers can be traced back to the 1970s. Koyama et al. [44] examined the velocity characteristics of rotating boundary layers by means of hot-wire anemometry and Pitot probes. Measurements were conducted along the spanwise centerline in a smooth straight channel at a fixed location under rotation. The thicknesses of the boundary layer and the wall friction factor were obtained by analyzing the measured velocity profile, which exhibited behaviors distinct from their stationary counterparts. The wall friction coefficient is larger than that in the flow without rotation.

Joubert and colleagues [45–47] also studied the turbulent boundary layer under the rotating state using hot-wire anemometers. Velocity was measured along the spanwise centerline in a smooth straight channel at different streamwise locations. Spatial resolution at $y^+=3$ was achieved to explore the flow evolution near the wall. The boundary layer thickness and wall friction coefficient were obtained. The viscous layer was found to be little affected by rotation, but the logarithmic region required a correction to account for the rotation effect. Such correction does not change the basic form of the logarithm law, except for the use of a different empirical coefficient. Unlike Koyama et al. [44], Joubert's group found that the wall friction coefficient decreases monotonically along the flow direction. At the same Reynolds number, the wall friction coefficient associated with the co-Coriolis surface is greater than its counterpart on a static wall, which in turn is greater than that of the counter-Coriolis surface. This observation was corroborated by Tao and colleagues [48–50] using more advanced measuring techniques.

In recent years, Tao et al. [15] developed an effective experimental technique based on hot-wire anemometer to simultaneously measure velocity and temperature. This method was specially designed for the study of boundary layers, as probes could be precisely positioned close to the wall at $y^+ = 1.8$, the highest resolution reported in the literature. They also studied, for the first time, non-isothermal boundary layers with temperature gradients. The normalized velocity distribution was found, as expected, to be shifted from its stationary counterpart due to the presence of the Coriolis force, as shown in Figure 7 for a

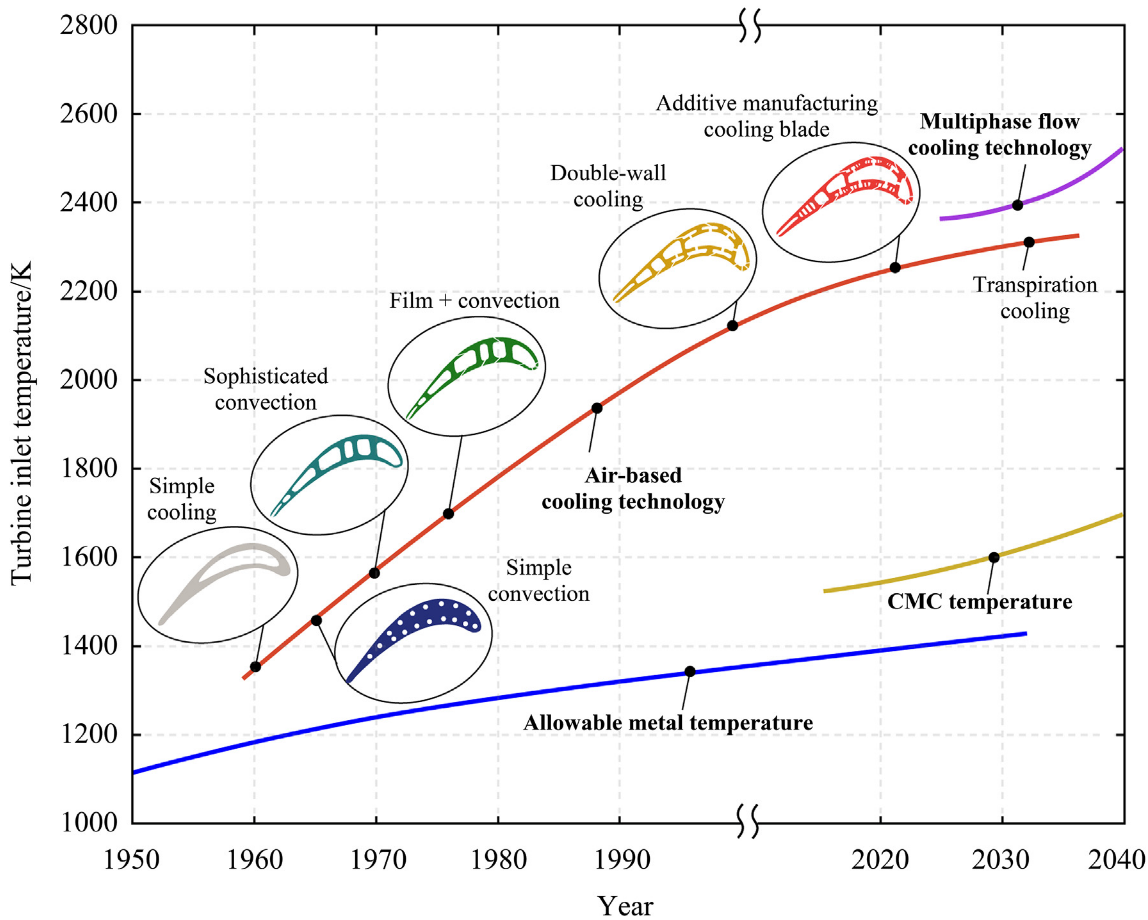

Figure 6 Evolution of turbine blade cooling technology (extended from Clifford [43]).

rotational speed of 120 rpm. Such a velocity shift depends upon the direction of rotation. For non-isothermal cases, buoyancy force was found to have clear effects on the velocity distribution. In the test conditions reported in Ref. [15], the buoyancy force weakens the Coriolis-force induced velocity change by up to 10%, as shown in Figure 8. New criteria to distinguish different flow regimes within rotating boundary layers were established, and the effects of rotation on the velocity and temperature profiles were identified. This work has extended classical boundary layer theory to include situations with rotation.

5.2. *Film cooling of turbine blade*

Film cooling, an external technique, has been widely used in advanced turbine blade design. It isolates hot

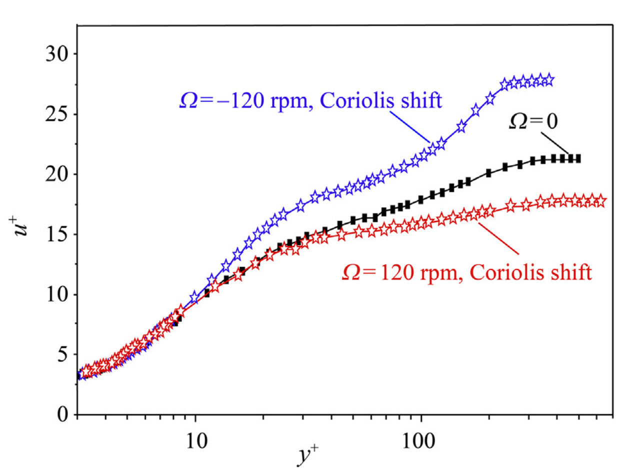

Figure 7 Velocity distribution in iso-thermal boundary layer under rotating conditions (Tao et al. [15]).

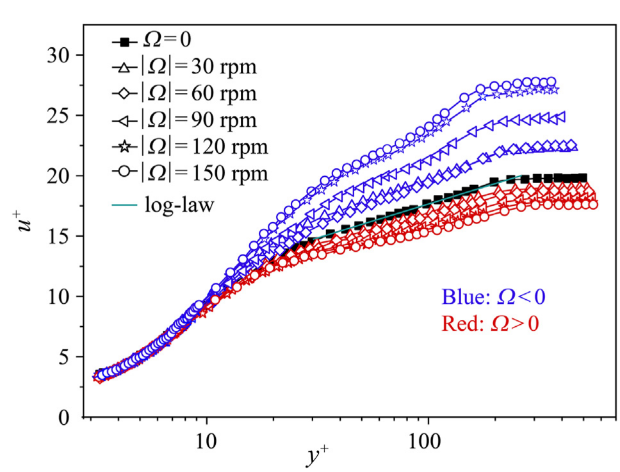

Figure 8 Comparison of velocity between iso-thermal and non-isothermal boundary layer (Tao et al. [15]).

combustion gases from the blade surface and significantly reduces blade surface temperature. Bunker [51] reviewed film cooling technologies as one of the few game-changing technologies to enable the high firing temperature in contemporary gas turbines. Since the 1960s, film cooling has been the subject of considerable research, and important results have been obtained based on studies in stationary wind tunnels. In contrast, few rotational experiments have been conducted, due to the challenges of measurement and data analysis. The cost of infrastructure development and maintenance has posed another serious concern. Since the performance of film cooling is significantly influenced by rotation, however, it is imperative to conduct relevant investigations under rotating conditions, regardless of the formidable challenges.

5.2.1. *Film cooling on flat surface*

The majority of early film cooling studies were carried out on a stationary flat plate. Bergeles et al. [52,53] were the first to enumerate the film cooling and flow characteristics of single hole on a flat plate, through a heat-mass transfer analogy method. Several factors that affect film cooling effectiveness were later explored, including hole geometry and flow conditions. Film cooling research based on a rotating flat plate, however, is relatively scarce. Young et al. [54] conducted numerical investigations, and concluded that the film coverage area decreases with increasing rotational speed. Al-Zurfi et al. [55] observed in their LES study that rotational speed is the dominant factor affecting film cooling performance on a rotating flat surface [56]. The film trace trajectory significantly deflects in the radial direction due to the high rotational speed. They further indicated that an anti-vortex hole provides better lateral film coverage downstream of the hole, with the benefit being more significant for a larger rotation number. Tao et al. [57] explored the effects of rotation direction on film coverage. The film trajectory was found to deflect from the centerline on both the suction and pressure sides, due to the combined influence of the Coriolis and buoyancy forces. Another interesting point is that the Coriolis force induced by deflection of the film trajectory has influence over the attachment of the film to the wall, as shown in Figure 9.

5.2.2. *Film cooling on curved surface*

Compared to film cooling on a flat surface, the situation on a turbine blade is extremely complex, because of the variation of curvature on a twist surface. The turbine blade surface can be divided into the suction surface, pressure surface, tip region, and endwall region. The suction surface has a convex shape and the pressure surface a concave shape. It is worth noting that the definitions of suction and pressure surfaces are different in the studies of film cooling, internal cooling, and compressor flow, due to differences in operation mode. Dring et al. [58] were the first to measure film cooling effectiveness on both the suction and pressure surfaces of a rotating blade. The temperature distribution was obtained using thermocouples and the film trajectory using ammonia dipstick. Li [59] conducted similar experiments. The roles of the Coriolis and centrifugal buoyancy forces in the determination of the film trajectory and coverage were characterized under a rotation condition.

Ahn et al. [60,61] investigated the film cooling characteristics of the leading edge of a rotating blade by means of a pressure sensitive paint (PSP) technique. A borescope was inserted between the guide vane and blade to provide optical access. Results indicated that the intake angle of the mainstream increases with increasing rotational speed. The stagnation region moves from the pressure to the suction side, leading to significant deflection of the film trace on the leading edge. Under off-design conditions, the deflection of film traces deteriorates film coverage. They also found that the area-averaged film cooling effectiveness is slightly improved with the increasing blowing ratio. Turbulence reduces the film cooling effectiveness at small blowing ratios, but exerts little effect at large blowing ratios. Moreover, a large blowing ratio leads to jet separation and enhanced mixing, thereby promoting the film coverage. Walters and Leylek [62] investigated the effect of hole configuration on film cooling performance. They found that a small spanwise angle improves film cooling effectiveness, but as the spanwise angle increases to 60°, the average effectiveness first increases and then gradually decreases with increasing blow ratio. The average cooling effectiveness of the leading edge decreases monotonically with an increase in hole spacing.

Gao et al. [63] studied the influence of mainstream intake angle in the blade tip region. The overall film cooling effectiveness varies slightly when the inlet flow angle changes within ±5°. Wang et al. [64,65] conducted a series of experimental and numerical investigations concerning the effect of mainstream vorticity and leakage flow on film cooling on the suction side in the tip region. Under rotation,

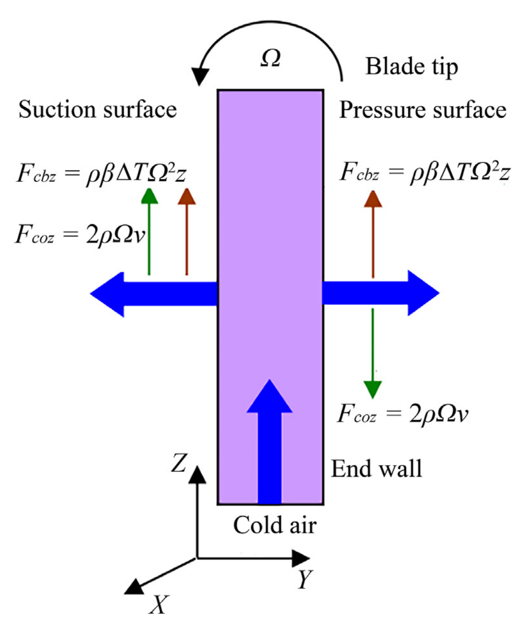

Figure 9 The action of Coriolis force and centrifugal buoyancy force on a rotating blade, from Tao et al. [57].

the squealer tip structure can change the leakage flow and weaken the passage vortex intensity, further affecting the film cooling performance in this region.

As compared with the blade surface and tip region, film cooling on the turbine endwall is even more challenging, mainly because the endwall has a complex three-dimensional contour and the film is affected by stronger passage vortices. Suryanarayanan et al. [66,67] investigated film cooling on the blade endwall of a three-stage turbine under rotation. The significance of the passage vortex was identified and emphasized. Rezasoltani and colleagues [68,69] studied the purge flow and film cooling of non-axisymmetric endwalls. The asymmetry of the endwall configuration significantly improves film cooling performance.

5.2.3. *Film cooling on turbine blade*

Turbine blades are usually equipped with multiple film holes. The geometry and layout of these holes must be optimized to provide the best film coverage and maximize the cooling performance. Ahn et al. [60,61] studied the effect of film hole layout on the cooling characteristics of turbine blades in an effort to compensate for the low cooling efficiency region between rows of holes and produce a more uniform coverage of the air film. Tao, Li, and colleagues [70−73] conducted a comprehensive investigation into the film cooling with multiple film holes in regions such as the leading edge and the suction and pressure surfaces. A non-orthogonal film hole layout was established to meet the cooling demands of turbine blades operating under realistic operating conditions. This method provides an effective means of improving film cooling effectiveness.

5.3. *Internal cooling in turbine blade*

Internal cooling is the earliest cooling method applied to turbine blades, dating back to the 1950s. It is achieved mainly through convective heat transfer in an optimized cooling structure. A variety of geometries have been studied and evaluated, including straight and U-shaped channels, lateral outflow column-rib channels, and impingement cooling, to cite a few. New schemes continue to be proposed.

5.3.1. *Straight channel under rotation*

The straight channel is the basic configuration for the study of internal cooling, and research on rotating straight channels commenced in the 1950s. Wagner and Johnson published a series of papers on rotating serpentine square channels in the 1990s [31−34], which are of milestone significance for the research in this topical area. They first applied the copper block method in rotation heat transfer experiments. Four dimensionless characteristic parameters, Reynolds number, density ratio, rotation number, and ratio of rotation radius to channel hydraulic diameter, were identified to characterize the heat transfer behaviors in rotating straight channels. Subsequent research mostly centered around the effects of these four dimensionless parameters, and on this basis, the influence of channel geometry was examined, including cross-section (square [74], rectangle [75], circle [31]), shape (straight channel [31], U-shaped channel [33]), and channel wall morphology (smooth channel [31], ribbed channel [32]). It was concluded that the Coriolis force enhanced heat transfer at the trailing edge of the channel, but the situation was reversed at the leading edge. The maximum enhancement and attenuation could be up to 50% within the range of experimental conditions.

Liou et al. [76−80] made significant contributions to the understanding of cooling channels. They studied the effects of rib structure, channel azimuth, aspect ratio, and other configurations on heat transfer in channels in order to simulate realistic internal cooling structures for practical turbine blades, and to develop empirical correlations for engineering applications. With the advancement of diagnostic technology, PIV and other measurement techniques were employed to study the flowfield in the channel, in order to reveal detailed flow physics and heat-transfer mechanisms. Tao and colleagues [81,82] used PIV to study the main and secondary flows in a rotating straight channel. Details of flow structures under the influence of Coriolis and buoyancy forces were visualized and key mechanisms were identified. Coletti et al. [20,83] used TR-PIV to explore the flow characteristics behind the ribs in rotating channels. Special attention was given to flow separation and its connection with the Coriolis and the buoyancy forces.

5.3.2. *U-turn channel under rotation*

Multi flow channels with U shapes are a commonly used cooling structure. The flow dynamics and cooling behaviors of a U-shaped channel are much more complicated than a straight channel. Liou et al. [84] used the transient liquid crystal technique to measure the distribution of heat transfer in a U-shaped channel, and found that rotation enhanced heat transfer intensity over the entire channel. In the turning section, the counter-vortex structure in the stationary condition becomes a large-scale single vortex under rotation. Turbulence in this region is significantly intensified, rendering enhanced heat transfer. Iacovides et al. [85−87] employed the LDV and liquid crystal techniques to measure the flow and heat transfer characteristics in a squared U-shaped channel. A large-scale single vortex was observed in the turning section under rotation. In addition, rotation significantly changed the development of the cross-sectional secondary flow in a radial inflow channel, which subsequently modified the velocity distribution and heat transfer in the channel. Similar experiments were performed by Gallo et al. [88−90]. They observed two hot spots with poor heat transfer within the second channel, appearing in the midstream and downstream regions near the medial side, respectively. The size and intensity of these hot spots increases as the rotation increases.

Parsons et al. and Zhang et al. [74,75,91] studied the effect of thermal boundary conditions on heat transfer in rotating ribbed channels. Under constant heat flow conditions, the heat transfer between the leading edge of the first process and the trailing edge of the second process of the ribbed channel was significantly higher than under constant wall-temperature conditions. Fu et al. [92] compared the thermal resistance and heat-transfer coefficients in channels with different aspect ratios ($1/4 \leq AR \leq 4$), and established similarity correlations.

Deng, Tao, and colleagues [93−97] explored the effects of structural parameters (channel aspect ratio, azimuth angle, and rib spacing, angle, and shape) and aerodynamic parameters (Reynolds, rotation, and buoyancy numbers) in ribbed U-shaped channels mimicking real cooling channels. Empirical laws for channel heat transfer were developed, and the flow physics and heat transfer processes were illuminated.

5.3.3. Wedge-shaped column-rib channel under rotation

Constrained by the shape of the blade, a lateral outflow column-rib channel is generally adopted to achieve effective cooling of the trailing edge. Willett and Bergles [98] performed early studies of the rotational heat transfer characteristics of a column-rib channel at the trailing edge. It was observed that the column-rib structure weakened the rotational effect, but could not completely eliminate its influence. Wright et al. [99,100] explored the heat transfer characteristics of rotating rectangular and wedge-shaped radial outflow channels with column ribs, with consideration of spoiler column materials. Liu et al. [101] studied the wedge-shaped smooth channel with lateral outflow, and found that the heat transfer in this configuration is stronger than in the radial outflow model. Rallabandi et al. [102] explored the flow and heat transfer characteristics of wedge-shaped channels with lateral outflow column ribs. The addition of the spoiler column significantly enhances heat transfer. The rotation effect increases the heat transfer on the trailing edge and weakens it on the leading edge. Qiu et al. [103] observed the phenomenon of critical rotation number in a rotating channel with wedge-shaped lateral outflow. The influence of rotation on the flow and heat transfer characteristics is reversed across the critical rotation number.

5.3.4. Impingement cooling under rotation

Impingement cooling is often used for the leading edge of turbine blades and in double-wall cooling structures that require intensive cooling. Early studies on impingement cooling under rotation were mainly carried out on models with radial impingement. Kreatsoulas [104] conducted detailed measurements of single-row jet impingement heat transfer under rotation in the 1980s. At a high rotation number, the heat transfer on the target surface could be reduced by 30%, compared with the stationary situation. Parsons and Han [105], Iacovides et al. [106], and Chiang and Li [107] also studied channels with jet impingement under rotation. Similar observations were made, that rotation reduced local heat transfer in jet-impinging channels. This phenomenon may be attributed to the Coriolis and centrifugal forces induced by rotation, which cause the jet to deviate from the target surface and reduced the cooling effectiveness. A judicious design is required to mitigate such deviation from the target surface by optimizing the impingement location and orientation. Several experimental studies [108−110] were performed to examine the effects of various geometrical parameters on cooling effectiveness. In general, rotation tends to enhance heat transfer for a relatively small impingement distance.

Multiple rows of impingement holes are a common configuration for turbine blade cooling. Yang et al. [111] found that the rotary pump effect enhanced heat transfer in the top region, with a maximum increase of 75%. Furlani et al. [112] noticed that rotation resulted in severe deflection of the jets, and the effect gradually decreased from high-radius to low-radius locations. Strong rotation may sometimes cause a reverse flow through the impingement hole at a low radius position. Studies by Deng et al. [113,114] revealed that channel rotation causes separation vortices to appear in the low-radius region. The phenomenon was enhanced with increase of the jet rotation number, leading to an uneven mass flow distribution and aggravating the difference in heat transfer between high and low radius locations.

5.4. Experimental cooling methods for turbine blades

5.4.1. Lamellar cooling

Lamellar cooling combines convective, impingement, and air film cooling, as shown schematically in Figure 10. It features a massive number of gaps and holes, designed to increase the area of heat transfer. The structure was first applied to cool stationary parts of a gas turbine, such as the combustion chamber and exhaust nozzle. In recent years, engineers have attempted to apply this structure to rotating blades; such efforts have been at small scale to date, but lamellar cooling may become a major direction for turbine cooling in the future [115]. The main parameters affecting the heat transfer characteristics of a laminate include the number of layers of the laminate, the opening rate, the distribution of holes, and the height and shape of the distribution column. Funazaki and colleagues [116,117] in their experimental study established correlations between the heat transfer coefficient and combined flow and geometric parameters. The pressure loss across the laminate was also obtained. Nakamata et al. [118] compared the effects of different blow ratios and proposed guidelines for structure design in terms of the blowing ratio (BR). At $BR < 0.5$, laminar units with a layout consisting of one air film hole, four spoiler columns, and one impact hole were found to have superior cooling performance. At $BR > 0.5$, the laminar unit with one air film hole, two spoiler columns, and one impact hole showed better performance. Land et al.

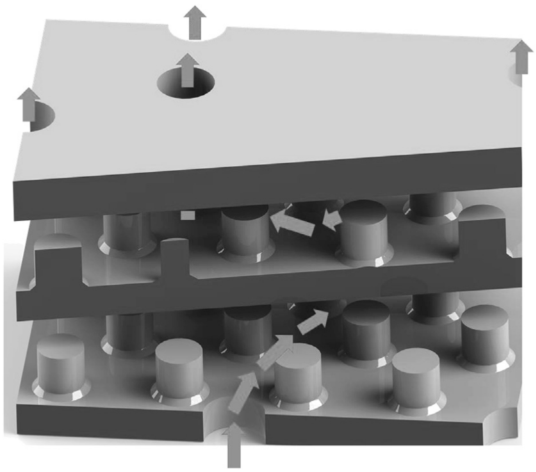

Figure 10 Schematic diagram of lamellar cooling structure, Bunker [115].

[119] investigated the effect of the relative positions of impact and film holes in a laminate structure on flow and heat transfer characteristics. A strong sensitivity of cooling effectiveness to the circumferential and radial placement of the impingement jet was observed. The jet-to-target distance played only a minor role.

5.4.2. Double-wall cooling

Double-wall cooling, as shown schematically in Figure 11 [120], is potentially a key cooling technology for aero-engine combustion chambers and turbine blades. Unlike lamellar cooling, it relies heavily on impingement cooling, an efficient cooling method depending on convective heat transfer. Ren et al. [121] conducted experimental investigations in which the structure of cross-flow air supply holes on the cold side were used to cool the plate. Results show that the adiabatic cooling efficiency is usually higher for lower Reynolds numbers at specific flow positions and blowing ratios. Convective heat transfer on the double-wall cooling structure was also investigated, with the air film holes arranged perpendicular to the main flow. Smaller impingement pitch and denser jet arrays provide better overall cooling effect.

5.4.3. Crater-structure enhanced cooling

The crater-structure enhanced cooling technology, as shown schematically in Figure 12, enhances heat transfer and reduces flow loss by means of an optimized arrangement of crater arrays on the wall surface. The heat transfer capacity of cold and hot channels with craters can reach 2−2.5 times that of smooth ones, but the pressure loss can also rise 2−4 times as the penalty [122]. Recent research on crater-enhanced cooling structures has focused on strengthening the heat transfer mechanism and reducing flow resistance.

Huang et al. [123] revealed the mechanisms of enhanced heat transfer due to the production of high Reynolds stress and turbulent kinetic energy when the air flows over the crater structures. Boundary layer separation occurs in regions with abrupt changes in the curvature of the crater [124]. The fluid away from the wall reattaches to the inner wall of the crater and forms a reattachment zone with a high heat transfer coefficient. The crater surface acts as a channel surface for strong convection or as an impingement surface to augment heat transfer. The heat transfer is further enhanced by the disturbance effect of the crater, which can be deployed in areas with high heat load. Anderson and Chapin [125] conducted convective heat transfer experiments using craters as the impingement surface, and found that crater spacing has a significant influence on the cooling efficiency. Kanokjaruvijit and Martinez-Botas [126] indicated that impingement cooling becomes more effective as the crater depth decreases. The total pressure loss is not sensitive to the structure of the impingement surface or the presence of the crater. The friction loss associated with the crater structure is limited.

5.4.4. Effusion cooling

Effusion cooling, as shown schematically in Figure 13, offers several advantages, including uniform cooling, broad film coverage, high cooling efficiency, easy control, and no deformation of the structure. Cold air is delivered to the hot stream through tiny injection holes (or porous material) and forms a protective cooling film on the blade surface. The blade material is of key significance in determining the cooling effectiveness of this method for practical applications. Greuel et al. [127] investigated the effusion cooling performance using C/C−SiC material as a thrust chamber liner for a cryogenic

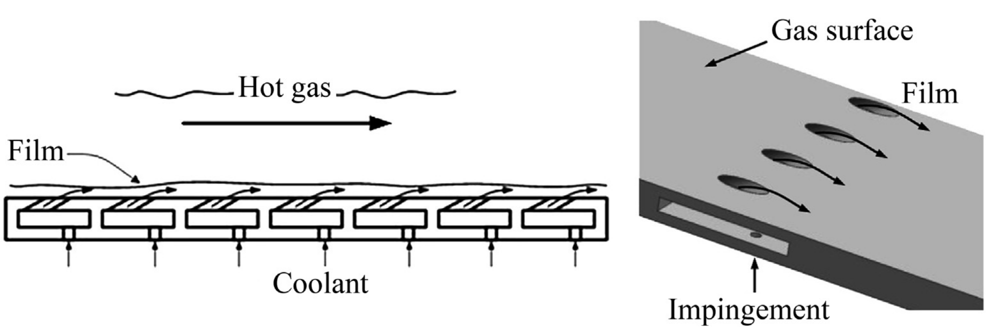

Figure 11 Schematic diagram of double-wall cooling, Wang et al. [120].

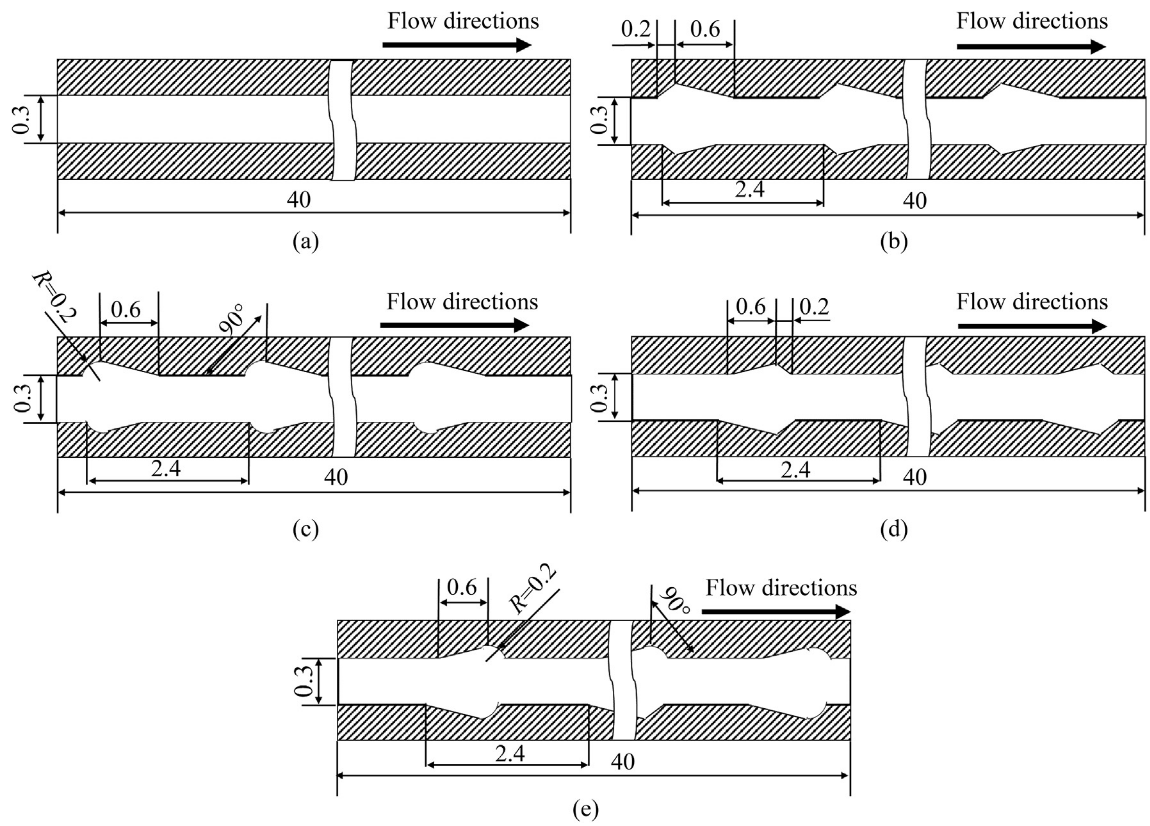

Figure 12 Schematic diagram of crater structures studied by Huang et al. [123]. (a) Straight channel; (b) triangle A; (c) a combination of 90° fan and triangle; (d) triangle B; (e) a combination of triangle and 90° fan (unit: mm).

liquid rocket engine. Results showed that only 0.7% of the main stream gas is sufficient for the cooling purpose. Herbertz et al. [128] utilized stainless steel sintered porous material as the skeleton material and experimentally investigated the effusion cooling characteristics for rocket engine combustion chambers and nozzles. New concepts continue to be proposed. For example, inspired by the transpiration phenomenon of trees, Jiang et al. [129] studied bionic effusion cooling and conceived a bionic self-extraction and adaptive effusion

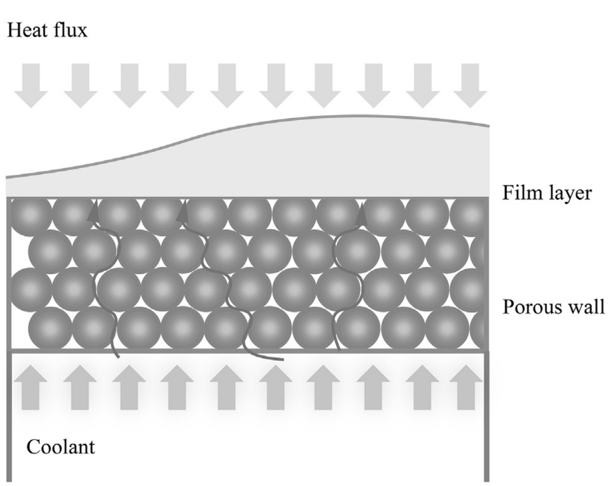

Figure 13 Schematic of effusion cooling structures studied by Jiang et al. [129].

cooling scheme for the leading-edge structures of certain types of hypersonic vehicles. These new concepts need to be further explored for practical application to turbine cooling.

6. Cooling of turbine disks

The flow physics in turbine disks are rich, and involve a variety of complex flow structures, including radial inflows, axial through flows, radial outflows, pre-swirled inflows, and flow through stator-rotor gaps. Extensive efforts have been made to develop appropriate, effective cooling methods that impose minimal flow losses. For rotating cavities in which the flow travels in the radial inward direction, Hide [130] first introduced a source-sink flow structure in the 1960s. Chew et al. [131] later utilized numerical simulation to investigate the source-sink flow in a rotating cavity which was assumed to be steady-state, axially symmetric, and isothermal. The distributions of the radial and circumferential velocities were calculated. Owen et al. [132] obtained the flow characteristics within free and rotating discs, and verified their theories against measured distributions of the axial flow, radial outflow, and radial inflow.

The circumferential velocity at the inlet of a rotating cavity is typically very high. A rigid vortex with high rotating velocity is generated in the cavity, giving rise to a severe pressure loss. A device known as a vortex reducer can be installed inside the cavity to reduce the inlet flow vorticity. Luo and colleagues [133,134] conducted flow measurements of various types of vortex reducers. The underlying mechanisms of flow losses were identified and guidelines for estimating these losses were established. The work provides a theoretical basis for optimization of the design of vortex reducers and rotating cavities.

The flow structure in an isothermal cavity with an axial inflow was first examined by Farthing et al. [135]. Air first enters the disk cavity along the radial arm. A portion of the air rotates in the same direction as the cavity, with the rest rotating in the opposite direction, forming counter-rotating circulation zones. Bohn et al. [136,137] conducted further research on the flow structure in the non-isothermal cavity proposed by Owen. In their numerical and experimental studies, Owen and colleagues [138−140] found that buoyancy can induce unstable flow. In the case of low Reynolds-number inlet flow, the buoyancy-induced effect is large, but it decreases for large Reynolds numbers. The same group performed a thermodynamic analysis [141,142], and a buoyancy model of the flow behaviors in rotating disk cavities was proposed. Owen [141] further derived the Ekman layer equation for a source-sink flow in an isothermal rotating cavity and applied it to buoyancy-induced flows. Owen conducted a review of the literature on buoyancy-induced flow in rotating cavities in 2015 [3].

Tian et al. [143] performed a numerical study of buoyancy-induced flow in a heated rotating cavity with an axial through-flow of cooling air. The Rayleigh-Bénard-like flow in a rotating system was carefully examined. The flow structure and heat transfer characteristics were found to be mainly controlled by the inertial, Coriolis, and centrifugal buoyancy forces. The Coriolis force alone does not affect the flow stability. It drives the flowfield to a steady state, while centrifugal buoyancy gives rise to flow instability.

Radial outflow in the turbine disc provides cooling air for the turbine blades and the high-pressure turbine disc cavity seals. There is often a pre-swirled nozzle at the cold air inlet of the rotating disc, for the purpose of reducing the total temperature and pressure loss of the cold air at the receiving hole. Two different flow patterns occur in the rotating-static disc cavity: the Batchelor [144] and Stewartson [145] flow patterns. They are mainly determined by the flow coefficient and the rotating Reynolds number. In 1969, Bayley and Owen [146] studied, both theoretically and experimentally, the influence of flow rate, rotational speed, and rotating-static clearance on the pressure and velocity fields, as well as the disc surface moment coefficient. Continued progress has been made over the past decades to improve the understanding of the internal flow dynamics and heat transfer of rotating-static disk cavities. Tang and Owen [147] and Jackson et al. [148] delineate recent developments.

7. Perspectives

Through nearly 70 years of development, basic cooling structures for the rotating components in gas turbines have been studied in detail. The present paper reviews some key topics; other areas of interest include structures with complex cross sections, combined structures, and new types of cooling structures. Advances in cooling technology for the high-temperature rotating components of gas turbines will not only facilitate the development of turbine products for industry and the design of aero-engine cooling structures, they will also enhance the academic community's understanding of flow and heat transfer mechanisms under rotation. The present review of past developments suggests three major directions for the future development of cooling technology for the high-temperature rotating parts of gas turbines. First, experimental research that closely aligns to practical cooling structures should be undertaken to obtain more realistic data to support engineering design. Complex structures face challenges in machining and testing, but the development of 3D printing and novel testing techniques will enable advances. Second, new cooling structures, such as micro-scale cooling and laminate cooling, should be explored. 3D printing will allow the construction of complex cooling structures. In addition, the cooling characteristics of these new structures will need to be studied, and techniques such as transient liquid crystals will make this possible. Third, the development of high-precision simulation methods and turbulence models is also crucial. In the future, high-fidelity simulation methods can be used in synergy with experimental data from near-real working conditions to realize accurate prediction of high-temperature rotating components and support the conceptualization and refinement of cooling designs for these parts.

References

[1] J.C. Han, S. Dutta, S. Ekkad, Gas Turbine Heat Transfer and Cooling Technology, second ed., CRC Press, Boca Raton, 2012.

[2] T.I. Shih, V. Yang, Turbine aerodynamics, heat transfer, materials, and mechanics, AIAA Progress in Astronautics and Aeronautics 243 (2014) https://doi.org/10.2514/4.102660.

[3] J.M. Owen, A.L. Christopher, Review of buoyancy-induced flow in rotating cavities, J. Turbomach. 137 (3) (2015) 031006.

[4] S. Acharya, Y. Kanani, Advances in film cooling heat transfer, Adv. Heat Tran. 49 (2017) 91−156.

[5] B. Weigand, B. Bonhoff, J.R. Ferguson, Comparative study between 2D boundary layer predictions and 3D Navier-Stokes calculations for a film cooled vane, in: ASME National Heat Transfer Conference, 1997.

[6] S. Neelakantan, M.E. Crawford, Prediction of film cooling effectiveness and heat transfer due to streamwise and compound angle injection on flat surfaces, in: Proceedings of the International Gas Turbine and Aeroengine Congress and Exposition, New York, USA, 1995.

[7] K.L. Miller, M.E. Crawford, Numerical simulation of single, double and multiple row film cooling effectiveness and heat-transfer, in: International Gas Turbine Conference and Exhibit, New York, USA, 1984.

[8] M.E. Crawford, W.M. Kays, R.J. Moffat, Full-coverage film cooling on flat, isothermal surfaces: data and predictions, NASA N3219, 1980.

[9] J.H. Leylek, R.D. Zerkle, Discrete-jet film cooling: a comparison of computational results with experiments, J. Turbomach. 116 (3) (1994) 358−368.

[10] M. Sivriolu, An analysis of the effects of pressure gradient and streamline curvature on film cooling effectiveness, Wärme-Stoffübertragung 26 (1991) 103−107.

[11] J.H.G. Howard, S.V. Patankar, R.M. Bordynuik, Flow prediction in rotating ducts using Coriolis-modified turbulence models, J. Fluid Eng. 102 (4) (1980) 456−461.

[12] C. Prakash, R. Zerkle, Prediction of turbulent flow and heat transfer in a radially square duct, J. Turbomach. 114 (4) (1992) 835−846.

[13] S. Dutta, M.J. Andrews, J.C. Han, Prediction of turbulent heat transfer in rotating smooth square ducts, Int. J. Heat Mass Tran. 39 (12) (1996) 2505−2514.

[14] J.Q. Zhu, Z. Tao, C.Q. Nie, Computational research on rotating channel by a modified anisotropic turbulence model, J. Therm. Sci. 20 (5) (2011) 385−393.

[15] Z. Tao, R.Q. You, Y. Ma, H.W. Li, Temperature and velocity characteristics of rotating turbulent boundary layers under non-isothermal conditions, Phys. Fluids 34 (2022) 065138, https://doi.org/10.1063/5.0096701.

[16] G.F. Li, H.W. Li, R.Q. You, H.J. Wu, Z. Tao, S.Z. Xia, Experimental investigation on velocity and temperature field in a rotating non-isothermal turbulent boundary layer using hot-wire, Sci. Rep. 10 (1) (2020) 9892.

[17] R. Gao, H.W. Li, R.Q. You, G.F. Li, S.Z. Xia, Hot-wire experimental investigation on turbulent Prandtl number in a rotating non-isothermal turbulent boundary layer, Propulsion and Power Research 9 (4) (2020) 317−325.

[18] F. Coletti, T. Maurer, T. Arts, A.D. Sante, Flow field investigation in rotating rib-roughened channel by means of particle image velocimetry, Exp. Fluid 52 (4) (2012) 1043−1061.

[19] F. Coletti, I. Cresci, T. Arts, Time-resolved PIV measurements of turbulent flow in rotating rib-roughened channel with Coriolis and buoyancy forces, in: Proceedings of ASME Turbo Expo, 2012, p. 553.

[20] F. Coletti, D. Lo Jacono, I. Cresci, T. Arts, Turbulent flow in rib-roughened channel under the effect of Coriolis and rotational buoyancy forces, Phys. Fluids 26 (4) (2014) 045111.

[21] J.M. Owen, Air-cooled gas-turbine discs: a review of recent research, Int. J. Heat Fluid Flow 9 (4) (1988) 354.

[22] C.L. Ong, J.M. Owen, Prediction of heat transfer in a rotating cavity with a radial outflow, J. Turbomach. 113 (1) (1991) 115−122.

[23] K. Wei, Z. Tao, H.J. Wu, G.Q. Xu, H.W. Li, R.Q. Rou, Interaction between the primary flow fields and the secondary flow fields under rotating condition, Exp. Therm. Fluid Sci. 84 (2017) 217−230.

[24] T.M. Liou, M.Y. Chen, K.H. Chang, Spectrum analysis of fluid flow in a rotating two-pass duct with detached 90° ribs, Exp. Therm. Fluid Sci. 27 (3) (2003) 313−321.

[25] S. Tomioka, S. Nishiyama, N. Miyamoto, D. Kando, S. Heshmat, Weighted reconstruction of three-dimensional refractive index in interferometric tomography, Appl. Opt. 56 (24) (2017) 6755−6764.

[26] B. Zhang, Z. Liu, W. Li, B. Luan, J. He, J. Dong, Characteristic visualization of the micro/mesoscale liquid ethanol diffusion flame by using deflection tomography, Int. Commun. Heat Mass Tran. 96 (2018) 43−52.

[27] J. Song, Y. Hong, M. Xin, G. Wang, Z. Liu, Tomography system for measurement of gas properties in combustion flow field, Chin. J. Aeronaut. 30 (5) (2017) 1697−1707.

[28] Y. Jin, Z. Guo, Y. Song, Z. Li, A. He, G. Situ, Sparse regularization-based reconstruction for 3D flame chemiluminescence tomography, Appl. Opt. 60 (3) (2021) 513−525.

[29] J.R. Osborne, S.A. Ramji, C.D. Carter, S. Peltier, S. Hammack, T. Lee, A.M. Steinberg, Simultaneous 10 kHz TPIV, OH PLIF, and CH_2O PLIF measurements of turbulent flame structure and dynamics, Exp. Fluid 57 (5) (2016) 65.

[30] X. Zhang, K. Wang, X. Wen, C. He, Y. Liu, W. Zhou, Experimental study of time-resolved simultaneous velocity and concentration fields of an inclined jet in crossflow, Int. J. Heat Mass Tran. 188 (2022) 122622.

[31] J. Wagner, B. Johnson, T. Hajek, Heat transfer in rotating passages with smooth walls and radial outward flow, J. Turbomach. 113 (1) (1991) 42−51.

[32] J. Wagner, B. Johnson, F. Kopper, Heat transfer in rotating serpentine passages with smooth walls, J. Turbomach. 113 (3) (1991) 321−330.

[33] B.V. Johnson, J.H. Wagner, G.D. Steuber, Heat transfer in rotating serpentine passages with selected model orientations for smooth or skewed trip walls, J. Turbomach. 116 (4) (1994) 738−744.

[34] B.V. Johnson, J.H. Wagner, G.D. Steuber, Heat transfer in rotating serpentine passages with trips skewed to the flow, J. Turbomach. 116 (1) (1994) 113−123.

[35] J.C. Han, Recent studies in turbine blade cooling, Int. J. Rotating Mach. 10 (6) (2004) 443−457.

[36] M.E. Taslim, A. Rahman, S.D. Spring, An experimental investigation of heat transfer coefficients in a spanwise rotating channel with two opposite rib-roughened walls, J. Turbomach. 113 (1) (1991) 75−82.

[37] S.V. Ekkad, Y. Huang, J.C. Han, Detailed heat transfer distributions in two pass square channels with rib turbulators and bleed holes, Int. J. Heat Mass Tran. 41 (23) (1998) 3781−3791.

[38] T.M. Liou, S.W. Chang, S.P. Chan, A. Lin, Influence of entrance geometry on flow field and heat transfer performance in stationary two-pass smooth parallelogram channels, Int. J. Heat Mass Tran. 105 (2017) 549−563.

[39] S.W. Chang, T.M. Liou, W.C. Chen, Influence of radial rotation on heat transfer in a rectangular channel with two opposite walls roughened by hemispherical protrusions at high rotation numbers, J. Turbomach. 134 (1) (2012) 011010.

[40] S.H. Jin, G.S. Kim, Simultaneous measurements of burning velocity and temperature distribution of combustion using UV laser Rayleigh scattering, Measurement 169 (2021) 108505.

[41] T.M. Liou, J.J. Hwang, Turbulent heat transfer augmentation and friction in periodic fully developed channel flows, J. Heat Tran. 114 (1) (1992) 56−64.

[42] S. Alaruri, T. Bonsett, A. Brewington, E. McPheeters, M. Wilson, Mapping the surface temperature of ceramic and superalloy turbine engine components using laser-induced fluorescence of thermographic phosphor, Opt Laser. Eng. 31 (5) (1999) 345−351.

[43] R.J. Clifford, Rotating heat transfer investigations on a multipass cooling geometry, AGARD CP 390, 1985.

[44] H. Koyama, S. Masuda, I. Ariga, I. Watanabe, Stability and destabilizing effects of Coriolis force on two-dimensional laminar and turbulent boundary layers, Journal of Engineering for Power 101 (1979) 23−29.

[45] J.H. Watmuff, H.T. Witt, P.N. Joubert, Developing turbulent boundary layers with system rotation, J. Fluid Mech. 157 (1985) 405−448.

[46] I. Macfarlane, P.N. Joubert, Effects of secondary flows on developing, turbulent, rotating boundary layers, Exp. Therm. Fluid Sci. 17 (1998) 79−89.

[47] T.B. Nickels, P.N. Joubert, The mean velocity profile of turbulent boundary layers with system rotation, J. Fluid Mech. 408 (2000) 323−345.

[48] K. Wei, Z. Tao, R.Q. You, H.J. Wu, H.W. Li, Development of a turbulent boundary layer in a rotating square cross-section channel with relatively high local rotation parameter, Exp. Therm. Fluid Sci. 86 (2017) 85−97.

[49] Z. Tao, H.J. Wu, H.W. Li, R.Q. You, G.F. Li, Rotation correction of wall function and velocity structure under the couple effects of buoyancy force and rotating effects at the entry section of the smooth straight channel, Int. J. Heat Fluid Flow 78 (2019) 108417.

[50] H.W. Li, Z.Y. Jiang, Z. Tao, R.Q. You, H.J. Wu, Effect of system rotating on turbulent boundary layer flow, Int. J. Heat Fluid Flow 75 (2019) 185−194.

[51] R.S. Bunker, A review of shaped hole turbine film-cooling technology, Journal of Heat Transfer Transactions of the ASME 127 (4) (2005) 441−453.

[52] G. Bergeles, A.D. Gosman, B.E. Launder, The near-field character of a jet discharged normal to a main stream, J. Heat Tran. 98 (3) (1976) 373−378.

[53] G. Bergeles, A.D. Gosman, B.E. Launder, Near-field character of a jet discharged through a wall at 30 deg to a mainstream, AIAA J. 15 (4) (1977) 499−504.

[54] P. Young, S.T. Ding, Z. Tao, Numerical Investigation of the Rotation on the Film Cooling over a Flat Surface, ASME Paper GT2005-68553, 2008.
[55] N. Al-Zurfi, A. Turan, A. Nasser, Numerical investigation of rotation effects on anti-vortex film-cooling holes, Flow, Turbul. Combust. 96 (1) (2016) 133−162.
[56] N. Al-Zurfi, A. Turan, LES of density ratio effects on film cooling under rotating frame, Heat Mass Tran. 52 (3) (2016) 547−569.
[57] Z. Tao, X.J. Yang, S.T. Ding, G.Q. Xu, H.W. Wu, H.W. Deng, X. Luo, Experimental study of rotation effect on film cooling over the flat wall with a single hole, Exp. Therm. Fluid Sci. 32 (5) (2008) 1081−1089.
[58] R.P. Dring, M.F. Blair, H.D. Joslyn, An experimental investigation of film cooling on a turbine rotor blade, J. Eng. Gas Turbines Power 102 (1) (1980) 81−87.
[59] G.Q. Li, Film Cooling Performance on Rotating Blades in 1.5-stage Turbine, Ph.D. Dissertation, Beihang University, Beijing, 2010.
[60] J. Ahn, M.T. Schobeiri, J. Han, H. Moon, Film cooling effectiveness on the leading edge region of a rotating turbine blade with two rows of film cooling holes using pressure sensitive paint, J. Heat Tran. 128 (9) (2006) 879−888.
[61] J. Ahn, M.T. Schobeiri, J. Han, H. Moon, Effect of rotation on leading edge region film cooling of a gas turbine blade with three rows of film cooling holes, Int. J. Heat Mass Tran. 50 (1−2) (2007) 15−25.
[62] D.K. Walters, J.H. Leylek, A detailed analysis of film-cooling physics: Part I — streamwise injection with cylindrical holes, J. Turbomach. 122 (1) (2000) 102−112.
[63] Z. Gao, D. Narzary, S. Mhetras, J.C. Han, Effect of inlet flow angle on gas turbine blade tip film cooling, J. Turbomach. 131 (3) (2009) 031005.
[64] H.C. Wang, Z. Tao, Z.Y. Zhou, F. Han, H.W. Li, Experimental and numerical study of the film cooling performance of the suction side of a turbine blade under the rotating condition, Int. J. Heat Mass Tran. 136 (2019) 436−448.
[65] H.C. Wang, Z. Tao, Z.Y. Zhou, H.M. Zhou, Y.W. Ma, H.W. Li, A study for the film cooling performance on the turbine blade suction side tip region under rotating conditions, Int. J. Heat Mass Tran. 138 (2019) 483−495.
[66] A. Suryanarayanan, B. Ozturk, M.T. Schobeiri, J.C. Han, Film-cooling effectiveness on a rotating turbine platform using pressure sensitive paint technique, J. Turbomach. 132 (4) (2007) 169−183.
[67] A. Suryanarayanan, S.P. Mhetras, M.T. Schobeiri, J.C. Han, Film-cooling effectiveness on a rotating blade platform, J. Turbomach. 131 (1) (2009) 37−47.
[68] M. Rezasoltani, M.T. Schobeiri, J.C. Han, Experimental investigation of the effect of purge flow on film cooling effectiveness on a rotating turbine with non-axisymmetric end wall contouring, J. Turbomach. 136 (9) (2014) 091009.
[69] M.T. Schobeiri, K. Lu, M. Rezasoltani, Effect of non-axisymmetric contouring on performance and film cooling of a rotating turbine endwall subjected to the secondary air purge: a combined numerical and experimental study, Proc. Inst. Mech. Eng. Part A Journal of Power and Energy 229 (A8) (2015) 813−831.
[70] H.W. Li, Z.Y. Zhou, G. Xie, S.Z. Xia, Z. Tao, The cooling performance of multiple rows of film holes on the suction surface of a turbine blade under rotating conditions, Appl. Therm. Eng. 188 (2021) 116125.
[71] Z.Y. Zhou, H.W. Li, G. Xie, S.Z. Xia, J.J. Zhou, The cooling performance of three-row compound angle holes on the suction surface of a rotating turbine blade, Propulsion and Power Research 10 (1) (2020) 23−36.
[72] G. Xie, Z. Tao, Z.Y. Zhou, R.Q. You, H.W. Li, Effect of leading edge diameter ratio and mainstream Reynolds number on film cooling performance of rotating blade leading edge, Appl. Therm. Eng. 186 (15) (2021) 116047.
[73] G. Xie, Z. Tao, Z.Y. Zhou, R.Q. You, S.Z. Xia, H. Li, Hole arrangement effect to film cooling performance on leading edge region of rotating blade, Int. J. Therm. Sci. 169 (2) (2021) 107034.
[74] J.A. Parsons, J.C. Han, Y.M. Zhang, Wall heating effect on local heat transfer in a rotating two-pass square channel with 90° rib turbulators, Int. J. Heat Mass Tran. 37 (1994) 1411−1420.
[75] J.A. Parsons, J.C. Han, Y.M. Zhang, Effect of model orientation and wall heating condition on local heat transfer in a rotating two-pass square channel with rib turbulators, Int. J. Heat Mass Tran. 38 (1995) 1151−1159.
[76] S.W. Chang, T.M. Liou, T.H. Lee, Heat transfer of a rotating rectangular channel with a diamond-shaped pin-fin array at high rotation numbers, J. Turbomach. 135 (4) (2013) 041007.
[77] T.M. Liou, Y.S. Hwang, Y.C. Li, Flow Field and Pressure Measurements in a Rotating Two-Pass Duct with Staggered Rounded Ribs Skewed 45degrees to the Flow, ASME Turbo Expo Paper GT2004-53173, 2004.
[78] T.M. Liou, M.Y. Chen, Y.M. Wang, Heat transfer, fluid flow, and pressure measurements inside a rotating two-pass duct with detached 90-deg ribs, J. Turbomach. 125 (3) (2003) 565−574.
[79] T.M. Liou, S.W. Chang, J.H. Hung, S.F. Chiou, High rotation number heat transfer of a 45° rib-roughened rectangular duct with two channel orientations, Int. J. Heat Mass Tran. 50 (19−20) (2007) 4063−4078.
[80] T.M. Liou, S.W. Chang, J.S. Chen, T.L. Yang, Y.A. Lan, Influence of channel aspect ratio on heat transfer in rotating rectangular ducts with skewed ribs at high rotation numbers, Int. J. Heat Mass Tran. 52 (23−24) (2009) 5309−5322.
[81] R.Q. You, H.W. Li, H.W. Wu, Z. Tao, PIV flow measurements for a rotating square smooth channel heated by basically uniform heat flux, Int. J. Heat Mass Tran. 119 (2018) 236−246.
[82] R.Q. You, H.W. Li, Z. Tao, K. Wei, Measurement of the mean flow field in a smooth rotating channel with Coriolis and buoyancy effects, J. Turbomach. 140 (4) (2018) 041002.1-041002.8.
[83] F. Coletti, T. Arts, Aerodynamic investigation of a rotating rib-roughened channel by time-resolved particle image velocimetry, Proc. IME J. Power Energy 225 (A7) (2011) 975−984.
[84] T.M. Liou, C.C. Chen, M.Y. Chen, TLCT and LDV measurements of heat transfer and fluid flow in a rotating sharp turning duct, Int. J. Heat Mass Tran. 44 (9) (2001) 1777−1787.
[85] H. Iacovides, D. Jackson, B. Launder, An experimental study of a rib-roughened rotating U-bend flow, Exp. Therm. Fluid Sci. 19 (3) (1999) 151−159.
[86] H. Iacovides, D.C. Jackson, G. Kelemenis, Experiments on local heat transfer in a rotating square-ended U-bend, Int. J. Heat Fluid Flow 20 (3) (1999) 302−310.
[87] H. Iacovides, D. Kounadis, Z.Y. Xu, Experimental study of thermal development in a rotating square-ended U-bend, Exp. Therm. Fluid Sci. 33 (3) (2009) 482−494.
[88] M. Gallo, T. Astarita, 3D reconstruction of the flow and vortical field in a rotating sharp "U" turn channel, Exp. Fluid 48 (6) (2010) 967−982.
[89] M. Gallo, T. Astarita, G.M. Carlomagno, Heat transfer measurements in a rotating two-pass square channel, Quantitative InfraRed Thermography Journal 4 (1) (2007) 41−62.
[90] M. Gallo, T. Astarita, G.M. Carlomagno, Thermo-fluid-dynamic analysis of the flow in a rotating channel with a sharp "U" turn, Exp. Fluid 53 (1) (2012) 201−219.
[91] Y.M. Zhang, J.C. Han, J.A. Parsons, C.P. Lee, Surface heating effect on local heat transfer in a rotating two-pass square channel with 60° angled rib turbulators, ASME Journal of Turbomachinery 117 (1995) 272−280.
[92] W.L. Fu, L.M. Wright, J.C. Han, Buoyancy effects on heat transfer in five different aspect-ratio rectangular channels with smooth walls and 45-degree ribbed walls, J. Heat Tran. 128 (11) (2006) 1130−1141.
[93] G.Q. Xu, Y. Li, H.W. Deng, Effect of rib spacing on heat transfer and friction in a rotating two-pass square channel with asymmetrical 90-deg rib turbulators, Appl. Therm. Eng. 80 (2015) 386−395.

[94] Y. Li, H.W. Deng, G.Q. Xu, Effect of Channel Orientation on Heat Transfer in Rotating Smooth Square U-Duct at High Rotation Number, ASME-IGTI Conference Paper GT2014-25188, 2014.

[95] Z. Tao, M.S. Yang, H.W. Deng, Heat transfer study in a rotating ribbed two-pass channel with engine-similar cross section at high rotation number, Appl. Therm. Eng. 106 (2016) 681−696.

[96] H.W. Li, R.Q. You, H.W. Deng, Z. Tao, J.Q. Zhu, Heat transfer investigation in a rotating U-turn smooth channel with irregular cross-section, Int. J. Heat Mass Tran. 96 (2016) 267−277.

[97] L. Qiu, H.W. Deng, J.N. Sun, Z. Tao, S.Q. Tian, Pressure drop and heat transfer in rotating smooth square U-duct under high rotation numbers, Int. J. Heat Mass Tran. 66 (2013) 543−552.

[98] F.T. Willett, A.E. Bergles, Heat transfer in rotating narrow rectangular pin-fin ducts, Exp. Therm. Fluid Sci. 25 (7) (2002) 573−582.

[99] L.M. Wright, W.L. Fu, J.C. Han, Thermal performance of angled, V-shaped, and W-shaped rib turbulators in rotating rectangular cooling channels (AR=4:1), J. Turbomach. 126 (4) (2004) 604−614.

[100] L.M. Wright, E. Lee, J.C. Han, Effect of rotation on heat transfer in rectangular channels with pin fins, J. Thermophys. Heat Tran. 18 (2) (2004) 263−272.

[101] Y.H. Liu, M. Huh, L.M. Wright, Heat transfer in trailing edge, wedge shaped cooling channels with slot ejection under high rotation numbers, Proceedings of the ASME Turbo Expo (2008) 311−320.

[102] A.P. Rallabandi, Y.H. Liu, J.C. Han, Heat transfer in trailing edge wedge-shaped pin-fin channels with slot ejection under high rotation numbers, J. Therm. Sci. Eng. Appl. 3 (2) (2011) 021007.

[103] L. Qiu, H.W. Deng, Z. Tao, Effect of Channel Orientation in a Rotating Smooth Wedge-Shaped Cooling Channel with Lateral Ejection, ASME Turbo Expo, GT2013-94758, 2013.

[104] J. Kreatsoulas, Experimental Data Cormelations for the Effects of Rotation on Impingement Cooling of Turbine Blades, AIAA Paper 1987-2008, 1987.

[105] J.A. Parsons, J.C. Han, Rotation effect on jet impingement heat transfer in smooth rectangular channels with heated target walls and radially outward cross flow, Int. J. Heat Mass Tran. 41 (13) (1998) 2059−2071.

[106] H. Iacovides, D. Kounadis, B.E. Launder, Experimental study of the flow and thermal development of a row of cooling jets impinging on a rotating concave surface, J. Turbomach. 127 (1) (2005) 222−229.

[107] H.W.D. Chiang, H.L. Li, Jet Impingement and Forced Convection Cooling Experimental Study in Rotating Turbine Blades, ASME Turbo Expo (2009) 679−689.

[108] E.Y. Jung, C.U. Park, D.H. Lee, J.S. Park, S. Park, H.H. Cho, ASME, Effect of rotation on heat transfer of a concave surface with array impingement jet, in: Proceedings of the ASME Turbo Expo: Turbine Technical Conference and Exposition, 2013.

[109] S.W. Chang, K.C. Yu, Thermal performance of radially rotating trapezoidal channel with impinging jet-row, Int. J. Heat Mass Tran. 136 (2019) 246−264.

[110] S.K. Hong, D.H. Lee, H.H. Cho, Heat/mass transfer in rotating impingement/effusion cooling with rib turbulators, Int. J. Heat Mass Tran. 52 (2009) 3109−3117.

[111] L. Yang, K. Tyagi, S. Ekkad, J. Ren, Influence of rotation on heat transfer in a two-pass channel with impingement under high Reynolds number, in: ASME Turbo Expo: Turbine Technical Conference and Exposition, 2015.

[112] L. Furlani, A. Armellini, L. Casarsa, Rotational effects on the flow field inside a leading edge impingement cooling passage, Exp. Therm. Fluid Sci. 76 (2016) 57−66.

[113] H.W. Deng, Z.S. Wang, J.S. Wang, H.W. Li, Flow and heat transfer in a rotating channel with impingement cooling and film extraction, Int. J. Heat Mass Tran. 180 (2021) 121751.

[114] H.W. Deng, H. Li, J.L. Xu, Heat transfer in an impingement cooling channel under isothermal boundaries at high rotation numbers, Int. J. Heat Mass Tran. 182 (2022) 121940.

[115] R.S. Bunker, Gas Turbine Cooling: Moving from Macro to Micro Cooling, ASME Turbo Expo, 2013.

[116] K. Funazaki, K. Hachiya, Systematic Numerical Studies on Heat Transfer and Aerodynamic Characteristics of Impingement Cooling Devices Combined with Pins, ASEM Turbo Expo, 2003.

[117] K. Funazaki, H.B. Salleh, Extensive Studies on Internal and External Heat Transfer Characteristics of Integrated Impingement Cooling Structures for HP Turbines, ASME Turbo Expo, 2008.

[118] C. Nakamata, F. Mimura, M. Matsushita, T. Yamane, T. Yoshida, Local Cooling Effectiveness Distribution of an Integrated Impingement and Pin Fin Cooling Configuration, ASME Turbo Expo, 2007.

[119] C.C. Land, C. Joe, K.A. Thole, Considerations of a double-wall cooling design to reduce sand blockage, J. Turbomach. 132 (3) (2010) 031011.

[120] K. Wang, H.W. Li, J.Q. Zhu, Experimental study of heat transfer characteristic on jet impingement cooling with film extraction flow, Appl. Therm. Eng. 70 (1) (2014) 620−629.

[121] Z. Ren, S.R. Vanga, N. Rogers, Internal and external cooling of a full coverage effusion cooling plate: effects of double wall configuration and conditions, Int. J. Therm. Sci. 124 (2018) 36−49.

[122] D.K. Hennecke, Turbine Cooling in Aeroengines, Von Karmen Inst. LS, 1982.

[123] B.H. Huang, H.W. Li, S.Z. Xia, Experimental investigation of the flow and heat transfer performance in micro-channel heat exchangers with cavities, Int. J. Heat Mass Tran. 159 (9) (2020) 120075.

[124] J.C. Han, L. Wright, Enhanced Internal Cooling of Turbine Blades and Vanes, NETL the Gas Turbine Handbook, 2006.

[125] A.M. Anderson, D.M. Chapin, The effects of dimpled surface geometry on heat transfer in an impingement jet flow, in: ASME International Mechanical Engineering Congress and Exposition, Paper IMECE2002-33718, 2002, pp. 73−79.

[126] K. Kanokjaruvijit, R.F. Martinez-Botas, Parametric effects on heat transfer of impingement on dimpled surface, J. Turbomach. 127 (2) (2005) 77−88.

[127] D. Greuel, A. Herbertz, O.J. Haidn, Transpiration Cooling Applied to C/c Liners of Cryogenic Liquid Rocket Engines, AIAA Conference Paper AIAA 2004-3682, Fort Lauderdale, Florida, 2004.

[128] A. Herbertz, M. Ortelt, I. Müller, Transpiration-cooled Ceramic Thrust Chamber Applicability for High-Thrust Rocket Engines, AIAA Paper 2012-3990, 2012.

[129] P.X. Jiang, G. Huang, Y. Zhu, Experimental investigation of biomimetic self-pumping and self-adaptive transpiration cooling, Bioinspiration Biomimetics 12 (5) (2017) 056002.

[130] R. Hide, On source-sink flows in a rotating fluid, J. Fluid Mech. 32 (4) (1968) 737−764.

[131] J.W. Chew, J.M. Owen, J.R. Pincombe, Numerical predictions for laminar source-sink flow in a rotating cylindrical cavity, J. Fluid Mech. 143 (1984) 451−466.

[132] J.M. Owen, J.R. Pincombe, R.H. Rogers, Source-sink flow inside a rotating cylindrical cavity, J. Fluid Mech. 155 (1) (1985) 233−265.

[133] Z.R. Liang, X. Luo, Y. Feng, G.Q. Xu, Experimental investigation of pressure losses in a co-rotating cavity with radial inflow employing tubed vortex reducers with varied nozzles, Exp. Therm. Fluid Sci. 66 (2015) 304−315.

[134] X. Luo, A. Feng, Y.K. Quan, Z.X. Zhou, N.B. Liao, Experimental analysis of varied vortex reducers in reducing the pressure drop in a rotating cavity with radial inflow, Exp. Therm. Fluid Sci. 77 (2016) 159−166.

[135] P.R. Farthing, C.A. Long, J.M. Owen, J.R. Pincombe, Rotating Cavity with Axial Throughflow of Cooling Air-Flow Structure, ASME Turbo Expo, 1990.

[136] D.E. Bohn, G.N. Deutsch, B. Simon, C. Burkhardt, Flow Visualization in a Rotating Cavity with Axial through Flow, ASME Turbo Expo, 2000.

[137] D. Bohn, J. Ren, C. Tuemmers, Investigation of the Unstable Flow Structure in a Rotating Cavity, ASME Turbo Expo, 2006.

[138] J.M. Owen, J. Powell, Buoyancy-induced flow in a heated rotating cavity, J. Eng. Gas Turbines Power 128 (1) (2006) 128−134.

[139] J.M. Owen, H. Abrahamsson, K. Lindblad, Buoyancy-induced flow in open rotating cavities, J. Eng. Gas Turbines Power 129 (4) (2007) 893−900.

[140] H. Tang, M.R. Puttock-Brown, J.M. Owen, Buoyancy-induced flow and heat transfer in compressor rotors, J. Eng. Gas Turbines Power 140 (7) (2018) 071902.

[141] J.M. Owen, Thermodynamic analysis of buoyancy-induced flow in rotating cavities, J. Turbomach. 132 (3) (2010) 1149−1158.

[142] J.M. Owen, H. Tang, Theoretical model of buoyancy-induced flow in rotating cavities, J. Turbomach. 137 (11) (2015) 111005.

[143] S. Tian, Z. Tao, S. Ding, G. Xu, Computation of buoyancy-induced flow in a heated rotating cavity with an axial throughflow of cooling air, Int. J. Heat Mass Tran. 51 (3−4) (2008) 960−968.

[144] G.K. Batchelor, Note on the class of solutions of the Navier-Stokes equations representing steady rotationally symmetric flow, Q. J. Mech. Appl. Math. 4 (1) (1951) 29−41.

[145] K. Stewartson, On the flow between two rotating coaxial disks, Proc. Camb. Phil. Soc. 49 (2) (1953) 333−341.

[146] F.J. Bayley, J.M. Owen, Flow between a rotating and a stationary disc, Aeronaut. Q. 20 (4) (1969) 333−354.

[147] H. Tang, J.M. Owen, Effect of radiation on heat transfer inside aeroengine compressor rotors, ASME Journal of Turbomachinery 143 (5) (2021) 051005.

[148] R.W. Jackson, H. Tang, J.A. Scobie, O.J. Pountney, C.M. Sangan, J.M. Owen, G.D. Lock, Unsteady pressure measurements in a heated rotating cavity, ASME Journal of Engineering for Gas Turbines and Power 144 (4) (2022) 041017.